SIN-CHN
SCIENTIFIC PRESS PTE.LTD.

Molecular & Cellular Biomechanics 2025, 22(4), 1184.
https://doi.org/10.62617/mcb1184

Article

Study of the effect of mechanical properties of materials on cell behaviour based on molecular dynamics simulations

Songjie Wu

Foundation Department, Liaoning Institute of Science and Technology, Benxi 117004, Liaoning, China; wsjys2004@163.com

CITATION

Wu S. Study of the effect of mechanical properties of materials on cell behaviour based on molecular dynamics simulations. Molecular & Cellular Biomechanics. 2025; 22(4): 1184.
https://doi.org/10.62617/mcb1184

ARTICLE INFO

Received: 19 December 2024
Accepted: 30 December 2024
Available online: 14 March 2025

Abstract: This study delves into the mechanical properties of polycrystalline tantalum nanomaterials with varying grain sizes and their influence on fibroblast behavior, utilizing molecular dynamics simulations. The cutting simulations revealed that tantalum nanomaterials with larger grain sizes exhibit superior mechanical performance. Detailed analyses of stress-strain curves, elastic modulus, and elongation at break further demonstrated that larger grain-sized tantalum nanomaterials possess enhanced toughness and compressive strength, positioning them as promising candidates for biomedical applications. Additionally, cellular experiments evaluated the biological effects of these nanomaterials on fibroblasts, showing that larger grain sizes significantly promote fibroblast proliferation. This highlights their potential in tissue engineering and regenerative medicine. By uncovering the intricate relationship between the mechanical properties of tantalum nanomaterials and cellular responses, this study underscores the critical role of material mechanics in biological applications and provides valuable insights for the future design of advanced biomedical materials.

Keywords: nanostructures; molecular dynamics; cellular behaviour; polycrystalline tantalum; fibroblasts

1. Introduction

The element tantalum is chemically stable, and as a transition metal with unique biocompatibility and mechanical strength, it has shown strong stability in long-term contact with the human body [1]. In the field of biomaterials, Tantalum stands out from the crowd of candidates due to its unique physical and chemical properties, offering significant advantages over other commonly used biomaterials such as titanium and cobalt-chromium alloys. First and foremost, biocompatibility is one of Tantalum's core strengths. Tantalum exhibits extremely high chemical stability in prolonged contact with human tissue, is not susceptible to oxidation or corrosion, and forms a good compatibility with the surrounding biological environment. This property significantly reduces the risk of inflammation, immune rejection or material degradation of the implanted material, making it more reliable in clinical applications. In contrast, while titanium and cobalt-chromium alloys are also biocompatible, they may suffer from passivation film rupture or localized corrosion in certain environments (e.g., chloride-containing or extreme pH environments), which can affect their biological performance.

Second, in terms of mechanical strength, tantalum is known for its excellent ductility and toughness. Tantalum's ability not only to withstand high mechanical loads, but also to maintain its structural integrity under large plastic deformations makes it particularly suitable for implants that are subjected to dynamic stresses. In contrast, titanium has high strength, but its relatively low ductility makes it susceptible

to fatigue fracture in areas of high stress concentration. Cobalt-chromium alloys, on the other hand, although having extremely high strength and hardness, have poor toughness and may suffer brittle fracture under certain circumstances. As a result, tantalum is considered an ideal material for medical implants that require long-term mechanical stability due to its balanced mechanical strength and toughness properties.

In addition, corrosion resistance is another outstanding feature of tantalum. The surface oxide layer formed by tantalum in physiological environments is extremely stable and dense, and is able to effectively resist chloride ion erosion in physiological fluids, exhibiting almost zero corrosion performance. This property allows for long-term stability in highly corrosive environments, such as joint fluids or salt ions in blood. In contrast, titanium, despite its passivation ability, may have its oxide layer destroyed under microscopic damage, leading to localized corrosion or pitting; and cobalt-chromium alloys, despite their corrosion resistance, may release metal ions, such as chromium or cobalt ions, from their surfaces, which may trigger a biotoxic or inflammatory response.

In summary, tantalum is not only widely used in medical fields such as orthopaedics, neurosurgery and cardiac stents, but its physicochemical stability also opens up new horizons for its application in tissue repair and regenerative medicine. As the "guardian" of metal implants, tantalum not only provides a stable physical environment for cells, but also promotes the integration of implants and human tissues with its unique mechanical properties. These advantages of tantalum are highly compatible with the research objectives and directions of the article, which is why it was chosen as the main research object of this paper. However, despite the success of tantalum in macroscopic applications, the mechanical properties of tantalum at the nanoscale and how these properties affect cellular behaviour remain to be further investigated.

At the nanoscale, matter takes on a very different appearance from the macroscopic world. Nanomaterials quietly bounce between molecules and atoms, exhibiting exotic mechanical and chemical properties. These properties make nanomaterials play a crucial role in modern technology, especially in biomedicine and tissue engineering. Research on nanomaterials has also been increasing, especially the effect of grain size on the mechanical properties of materials, which has become an important research direction in the field of nanomaterials [2]. With the decreasing grain size, nanomaterials, due to their large specific surface area and small grain size, usually exhibit very different physical behaviour from conventional materials in terms of mechanical, thermal and electrical properties: higher strength, better electrical conductivity and even more significant surface effects. In polycrystalline materials, the presence of grain interfaces not only shapes the strength and toughness of the material, but also determines the deformation mechanism of the material under stress. Especially at the nanoscale, these interfaces become exceptionally active, greatly enhancing the material's ability to respond to external forces. Therefore, the study of the microstructure of nanomaterials, especially the relationship between grain scale and mechanical properties, has become a hot spot in the academic community to further deconstruct the properties of materials.

The mechanical properties of polycrystalline tantalum materials undoubtedly present a completely new look at the nanoscale. Through molecular dynamics

simulation (MD), we are able to deeply explore its deformation mechanism at the microscopic scale [1]. MD is a technique to calculate the dynamic evolution of molecular systems through numerical methods based on classical mechanics principles, which is widely used to study the microstructure and mechanical properties of substances, etc., especially at scales difficult to be directly observed by experiments to provide an important Theoretical basis. At the nanoscale, the "mechanical soul" of a material is not only dependent on macroscopic external forces, but also closely related to grain size, grain boundary behaviour and interatomic interactions. The strength of tantalum at the nanoscale results from the precise coordination of each atom and grain boundary.

Although tantalum, as a metallic material with excellent biocompatibility, has been widely used in many biomedical fields, there is still a lack of systematic studies on its mechanical properties at the nanoscale and the specific effects of these properties on cellular behaviours [3]. An in-depth analysis of the mechanical properties of polycrystalline tantalum nanoparticles will not only advance the research process in the field of materials physics, but will also provide a breakthrough in the field of cell behaviour regulation. Cells perceive the material and respond biologically accordingly. The hardness, toughness and distribution of the stress field of polycrystalline tantalum nanomaterials will affect biological processes such as cell proliferation, differentiation and migration through the cellular mechanosensing system. And cell behaviour, especially cell proliferation, is an important topic of research in the biomedical field [4]. Fibroblasts among various types of cells are the widespread stromal cells in the organism, which are mainly involved in the repair and remodelling of tissues, and they are an important target for the study of cell proliferation behaviour. It has been shown that the micro-mechanical environment of materials plays an important role in the proliferation of fibroblasts.

There is not enough scientific evidence to explain how the grain size of polycrystalline tantalum nanomaterials and their mechanical properties affect cell proliferation and differentiation. Therefore, this study aims to delve into the mechanical properties of polycrystalline tantalum nanomaterials with different grain sizes through molecular dynamics simulations and to explore how these mechanical properties can further reveal the intrinsic mechanisms of cell-material interactions by affecting cell behaviour.

2. Simulation process and methodology

2.1. Modelling

In this study, the experiments of cutting simulation are crucial; the mechanical properties of polycrystalline tantalum nano with different grain sizes directly affect the surface properties of the material during the cutting process [5]. These surface properties in turn play an important role in the material-cell interaction, which in turn affects biological behaviours such as cell attachment and proliferation. Therefore, the effect of grain size on the surface morphology and its mechanical response of tantalum materials can be comprehensively revealed through cutting simulation, which provides the necessary physical background for subsequent biological studies and the

theoretical basis for an in-depth exploration of its cellular response mechanism.

To minimize variability and ensure reproducibility in the material preparation process, several measures were implemented to standardize the model construction and simulation setup. The atomic-level model of polycrystalline tantalum was constructed using the Voronoi method integrated into the Atmosk software, with strict adherence to tantalum's lattice constants (a = 0.3234 nm, c = 0.5168 nm) to maintain its body-centered cubic (BCC) crystal structure [6]. To further enhance consistency, random number generators were used with fixed initialization seeds, ensuring reproducible grain structures across simulations [7]. The material dimensions (Lx = 30 nm, Ly = 6 nm, Lz = 15 nm) and atom count (191,955 atoms) were consistently maintained, with periodic boundary conditions applied in the Y-direction to eliminate edge effects and accurately simulate bulk material behavior.

The polycrystalline tantalum was divided into three distinct layers: the fixed layer, thermostatic layer, and Newtonian layer. The fixed layer, located at the base of the material with a thickness of 1 nm, was constrained to maintain atomic stability and simulate substrate interactions. Adjacent to this, the thermostatic layer (1 nm thick) was temperature-controlled using the Nosé-Hoover thermostat, ensuring stable heat transfer and equilibrium during the cutting process. The remaining atoms formed the Newtonian layer, where atomic motions were determined strictly by interatomic forces under Newton's second law. Similarly, the diamond cutting tool was divided into fixed, thermostatic, and Newtonian layers, with precise thicknesses of 0.5 nm for the fixed and thermostatic layers, and positioned 0.5 nm from the material's boundary to standardize the initial tool-material interaction.

Grain orientation and distribution were randomized using controlled algorithms, with fixed random seeds to simulate natural polycrystalline variability while ensuring reproducibility. The spherical grain distribution assumption was validated against experimental data to confirm its fidelity to real-world polycrystalline structures. Additionally, thermal and mechanical conditions were tightly regulated, with the thermostatic layer maintaining a constant temperature of 300 K and cutting speed, tool trajectory, and external forces standardized across all simulations. Energy minimization and system relaxation steps (100,000 iterations) under an NVT (canonical ensemble denotes a system with a definite number of particles (N), volume (V), and temperature (T), abbreviated as NVT) ensemble were performed to eliminate high-energy configurations and ensure equilibrium.

Finally, surface boundary conditions were carefully defined. Periodic boundary conditions were applied in the Y-direction to simulate infinite material continuity, while non-periodic conditions in the X and Z directions allowed for free material deformation during cutting. These measures collectively reduced variability and ensured the results were robust, reproducible, and reflective of tantalum's intrinsic mechanical and thermal properties under controlled conditions.

In this study, in order to simplify the model and maintain its scientific validity, a spherical distribution of grains is assumed, an assumption that is in line with common practice in many materials science studies, and which can effectively reduce computational complexity and facilitate analysis. The size of the grains (d_g) is expressed through their average diameter, and this size is usually considered as one of

the important characteristics of the grain scale in polycrystalline materials [8]. The specific calculation formula is given below:

$$d_g = 2\sqrt[3]{\frac{3N_{ave}V_x}{4\pi}} \tag{1}$$

where N_{ave} is the average number of Ta atoms contained in the grain and V_x is the volume of Ta atoms calculated using the Voronoi method.

2.2. Selection of potential functions

In the molecular dynamics simulation of this study, the Morse potential function [9] was chosen to accurately describe the interaction force between the diamond tool and the tantalum material. The Morse potential function is an empirical potential function that is widely used in the interaction between atoms and molecules, and it is particularly suitable for modelling short-range interactions. During the cutting process, the interaction forces between diamond tools and tantalum materials show strong short-range characteristics, especially in the contact region. The Morse potential function can effectively capture this characteristic and accurately describes the mutual attraction and repulsion forces between atoms through its asymmetric potential energy curves, which is particularly suitable for the complex interactions between tantalum and diamond materials. The functional form is as follows:

$$U(r_{ij}) = D_0\left[e^{-2\alpha(r_{ij}-r_0)} - 2e^{-\alpha(r_{ij}-r_0)}\right] \tag{2}$$

where D_0 and α are the atomic binding energy and elastic modulus of the Morse potential, respectively; r_0 denotes the equilibrium distance between atoms i and j; r_{ij} denotes the equilibrium distance between atom i and atom$j$ the distance between atom i and atom j. The parameters are D_0 = 1.56eV, α = 3.3786 Å^{-1}, and r_0= 2.1187Å.

In this paper, the Tersoff potential function has been chosen to describe the interactions between atoms inside a diamond tool [10]. The Tersoff potential function is a potential function commonly used to describe the interactions between atoms in covalent materials, and is particularly suited to describing materials with strong covalent bonds such as diamond. The ability of this potential function to accurately model short- and medium-range interactions between atoms and to take into account the effect of the atomic environment on the mechanical behaviour gives it a significant advantage when modelling interatomic interactions within diamond tools. Its specific expression is given below:

$$U_{ij}(r_{ij}) = \frac{1}{2}\sum_i \sum_{i\neq i} f_C(r_{ij})\left[a_{ij}f_R(r_{ij}) + b_{ij}f_A(r_{ij})\right] \tag{3}$$

$$f_C(r_{ij}) = \begin{cases} 1 & ,r < R - D \\ \frac{1}{2} - \frac{1}{2}\sin\left(\frac{\pi}{2}\frac{r-R}{D}\right), & R - D < r < R + D \\ 0 & ,r > R + D \end{cases} \tag{4}$$

$$f_R(r_{ij}) = Ae^{-\lambda_1 r} \tag{5}$$

$$f_A(r_{ij}) = -Be^{-\lambda_2 r} \tag{6}$$

where: $f_C(r_{ij})$ is the truncation function, in order to concentrate on the short-range interaction forces with significant contributions, limit the range of interatomic interactions calculated, and improve the efficiency of the calculation, we only consider the $R + D$ truncationrange of interatomic forces; a_{ij} is the repulsion coefficient and b_{ij} is the attraction coefficient, which regulate the strength of interatomic interactions, controlling the magnitude of the repulsive and attractive forces, respectively; $f_R(r_{ij})$ and $f_A(r_{ij})$ calculate the repulsive and attractive interaction forces, respectively. Based on experimental data and theoretical studies of diamond materials the parameters were determined as A = 1393.6eV, B = 346.7eV, λ_1 = 3.4879Å^{-1}, λ_2 = 2.2119Å^{-1}.

In this paper, the interactions between tantalum atoms are described using the embedded atom method (MEAM) potential function, which is a classical force-field model widely used in metal and alloy systems, and is paticularly suitable for describing the interaction forces between atoms in metallic materials, drawing on the study of [11]. Compared with the conventional embedded atom model (EAM), the MEAM potential function is able to take into account the directional effects and many-body interactions between atoms more accurately, and thus has significant advantages when modelling metallic materials with complex crystal structures such as tantalum. Its expression is as follows:

$$U_{ij}(r_{ij}) = \sum_{i<j} \phi(r_{ij}) + \sum_i U(n_i) \tag{7}$$

$$n_i = \sum_j \rho(r_{ij}) + \sum_{j<k} f(r_{ij}) f(r_{ik}) g[cos(\theta_{jik})] \tag{8}$$

where: $\phi(r_{ij})$ denotes the short-range pair of potentials between atoms, which describes the interaction force between two atoms due to their close proximity. This pair potential is usually used to model the direct contact interaction between atoms, including repulsive and short-range attractive forces, which play a dominant role especially when the distance between the atoms is small; U_{ij} represents the potential between atoms i, j, which takes into account the energetic contribution of the interaction between these two atoms; r_{ij} is the distance between atoms i and j, which represents the relative position of the two atoms in space; the parameter θ_{jik} represents the energy contribution of the interaction between the two atoms centered at atom i, k, and the energy contribution of the interaction between the two atoms. j, k the angle between them. This term takes into account the directional effects between atoms, especially in materials such as metals and alloys, where interatomic interactions are often not only dependent on distance, but are also affected by relative orientation. By introducing this angle term, the MEAM potential function is able to more accurately characterize the anisotropy of materials such as tantalum. After the interatomic interaction forces have been determined, the state of motion of each atom in the system can be calculated by solving the Newton equation. Newton's equation describes the law of motion of atoms under force in the form:

$$m_i \frac{d^2 L_i}{dt^2} = F_i \tag{9}$$

where m_i is the mass of atom i, L_i is the position vector of atom i, and F_i is the total force on atom i.

3. Simulation results

3.1. Molecular dynamics simulations (selected grain size: dg = 8.72 nm)

In this paper, the molecular dynamics simulation was performed using the open source software Lammps [12]. If the initial model is unreasonable and the distance between atoms is too close, it is easy to lead to a system with too high energy and too fast atoms. In this paper, a default optimisation algorithm (quasi-Newton algorithm) is used for energy minimisation to eliminate uncertainties in the modelling process. The system is relaxed 100,000 steps using the NVT system, and the time step is set to 1 fs, so that the total energy of the system is minimised and the equilibrium temperature of 300K is reached, and all of them fluctuate within a small range. After the start of cutting, the NVE (micro-canonical ensemble, denoted with a definite number of particles (N), volume (V), and energy (E), abbreviated as NVE) system was selected for the Newtonian layer and the NVT system was used to control the temperature of the thermostatic layer. In this paper, the internal plastic deformation of the workpiece during the cutting process was analysed with the help of Dislocation Extract Analysis and Atomic Strain Analysis in the visualisation software Ovito [13,14].

During the initial stages of cutting, the cutting forces are almost zero. This is due to the fact that the separation distance between the tool and the material is greater than the critical radius of their interaction, resulting in no significant interaction force between the two. As the cutting process advances, the tool begins to approach the material surface, and Van der Waals gravity gradually forms between the tool and the material atoms, at which time both the tangential force Fx and the normal force Fz exhibit negative values, indicating that the material undergoes preliminary microscopic deformation under the action of the cutting force.

As the tool continues to feed, the contact surface gradually increases and the interaction force between the material and the tool gradually increases, which in turn leads to the cutting phase. During this process, the atomic layer on the material surface is forced to slip or fracture, thus initiating the cutting behaviour. At this time, the cutting force will gradually increase with the increase of the cutting distance, and shows a typical non-linear growth trend. The cutting force at this stage is influenced by multiple factors such as material hardness, cutting speed and tool geometry.

The workpiece first experiences elastic deformation during the cutting process, and with the gradual increase in deformation, the cutting energy is converted into strain energy and stored in the lattice structure of the material. After the lattice deformation, the chips formed accumulate in the front of the tool, and the chip volume increases rapidly, resulting in a sharp increase in cutting force. When the cutting depth of the tool reaches 4 nm, the cutting process enters a stabilisation stage, but the cutting force still shows some fluctuations. The main reasons for the fluctuation of cutting force can be attributed to the complex physical processes such as lattice deformation, lattice

reconstruction, nucleation and expansion of defect structures, and absorption and release of lattice strain energy. Specifically, the lattice undergoes irreversible deformation during the cutting process, and localised regions may produce defective structures (e.g., dislocations and vacancies), which further affect the mechanical properties of the material.

During the cutting process, the tangential force (Fx) and cutting force (F) still show a gradual increase in the stabilization phase, which is closely related to the accumulation of cutting energy. With the deepening of the cutting process, the phenomena of dislocation nucleation, entanglement and obstruction become more significant, which leads to work hardening of the material and thus increases the deformation resistance of the material. At the same time, as the temperature of the workpiece increases, the material begins to undergo thermal softening effects, and the hardness and cutting force of the material gradually decrease. In addition, the presence of grain boundaries also has an effect on the cutting force, especially in materials with smaller grain sizes, the hindering effect of grain boundaries on the cutting force is more obvious, which further increases the amplitude of the fluctuation of the cutting force.

The combined effect of strain rate hardening, thermal softening and grain boundary effect plays a decisive role in the variation of cutting forces. The reason for the fluctuating change in the normal force (Fz) is due to the difference in the interaction force between the chip at the front tool face and the atoms below the back tool face during the cutting process. The chip atoms located on the front face exert a downward force on the tool, while the atoms located below the back face exert an upward force, and this difference in force makes the normal force (Fz) fluctuate during the cutting process. With the continuous accumulation of chip atoms on the front face, the direction and magnitude of the cutting force will keep changing with the advancement of the accumulation process, which leads to the fluctuating change of the normal force (Fz). In the cutting process, the tangential force (Fx) is usually larger than the normal force (Fz), which indicates that the shear effect dominates in the stable cutting stage, while the extrusion effect is relatively small. Since the forces exerted by the workpiece on both sides of the tool are in equilibrium, the transverse force (Fy) fluctuates around the value of 0, reflecting the mechanical equilibrium and deformation mechanism in the cutting process.

In the stable cutting stage, the average cutting force under this condition is characterized by calculating the average value of the cutting force, and the influence law of grain size on the average cutting force is analyzed, as shown in **Figure 1**. The results show that the average cutting force F' increases significantly with the decrease of the workpiece grain size. The grain size has an important effect on the mechanical properties of metallic materials, and the finer the grain size, the harder and stronger the material will increase accordingly. This is mainly attributed to the blocking effect of grain boundaries, which act as barriers to the movement and diffusion of dislocations in metallic materials and will effectively hinder the slip of dislocations, increasing the deformation resistance of the material, which leads to a rise in the average cutting force F'. In addition, both the average tangential force and the average normal force show a certain degree of volatility, which is mainly closely related to factors such as the crystal orientation of the workpiece and the location and density of

the grain boundaries. The average transverse force, on the other hand, shows fluctuating changes around the zero line and reaches its maximum value at a grain size of 5.93 nm, indicating that the cutting state is the most unstable at this time, which may be due to the inhomogeneity of the local deformation of the material caused by the increase in the density of the grain boundaries, which further aggravates the fluctuation of the cutting force. Overall, although the grain size reduction can improve the material strength, it also increases the complexity and instability of the cutting process.

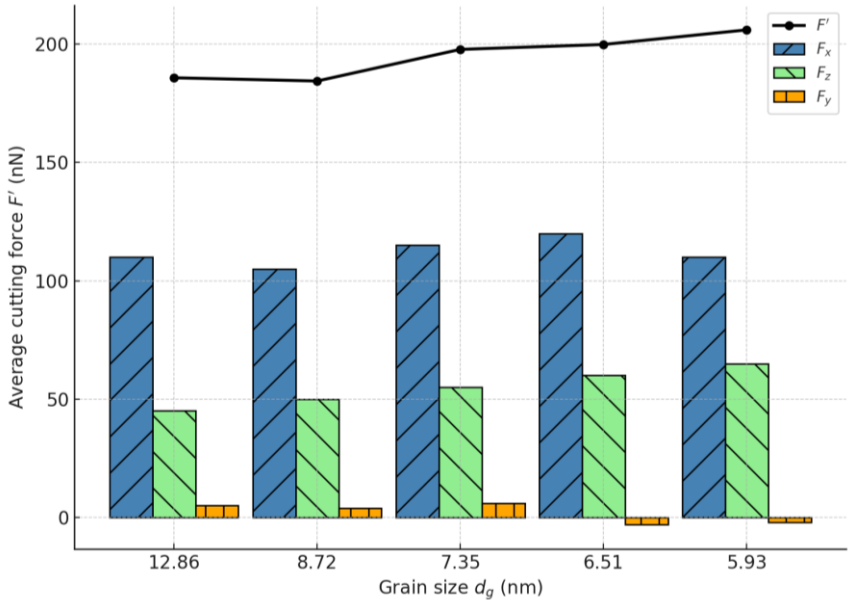

Figure 1. Effect of grain size on average cutting force.

At the end of cutting, the temperature distribution of workpieces with different grain sizes shows typical heat accumulation characteristics. There are three main heat-generating regions during the cutting process: the shear surface, the contact zone between the chip and the front face, and the contact zone between the back face and the transition surface. These three heat generating regions correspond to the three deformation zones in the cutting process [15]. Therefore, the source of cutting heat mainly consists of the plastic deformation work of the chips and the friction work on the front and rear tool faces. It is worth noting that the highest temperatures on the front and back tool surfaces do not occur at the cutting edge, but are located on the outer surface of the chip at some distance from the cutting edge, which is due to the conduction and accumulation of heat inside the material.

At the beginning of the cutting process, there is a slight decrease in the temperature of the workpiece, which is caused by the initial gap of about 0.5 nm between the tool and the workpiece. Before the tool touches the workpiece, the ambient temperature is 300 K, while the initial temperature of the workpiece is 335 K, which is higher than the ambient temperature, so there is a heat exchange between the workpiece and its surroundings, which leads to a slight decrease in temperature. As the tool comes into contact with the workpiece, the cutting process begins and the heat of friction and material deformation rapidly accumulates in the cutting zone, leading to a significant increase in the workpiece temperature. The temperature increase not

only reflects the cutting energy consumption and transformation, but also closely related to the grain size, friction contact area and the thermal conductivity of the material.

3.2. Surface roughness

Surface roughness is a key indicator for evaluating the surface quality of workpieces, which is especially important in the field of precision manufacturing and nano-cutting [16]. In the nano-cutting process, due to the dual action of high temperature and high pressure in the contact area between the workpiece and the tool, significant plastic deformation occurs within the material, resulting in crystal defects such as dislocations and vacancies. The density of grain boundaries plays a crucial role in this process, as higher grain boundary density can inhibit dislocation motion by acting as barriers, thereby increasing material strength and altering stress distribution within the material. These stress concentrations at grain boundaries not only influence the mechanical behavior of the material but also affect cellular mechanotransduction when interacting with biological systems. During cutting, these crystal defects continue to expand and migrate, leading to the micro-reconstruction of the material's structure in the local region, further influencing surface roughness and its impact on both mechanical and biological performance. With the advancement of tool cutting, the high temperature and high pressure in the cutting area make the crystal lattice on the surface of the workpiece in a high stress state. When the tool passes through the cutting region, the lattice structure of the workpiece relaxes, which causes partial elastic recovery. In this process, the rebound effect of dislocations leads to the formation of microscopic atomic steps on the surface of the workpiece, and these steps stack and accumulate to form the surface roughness. In addition, factors such as the elastic-plastic properties of the material, grain size, cutting speed and tool shape all have an important influence on the surface roughness.

In this paper, surface roughness is quantified and evaluated by the root-mean-square deviation (Rq) of the three-dimensional surface profile [17]. Rq as a statistical characterization parameter, can effectively reflect the root-mean-square (RMS) value of the surface height deviation and comprehensively describe the degree of fluctuation of the surface microform. This quantitative method helps to deeply understand the influence of different grain sizes, cutting parameters and tool conditions on surface quality, and provides theoretical basis and data support for improving the precision and efficiency of nano-cutting process. The specific formula is as follows:

$$Rq = \sqrt{\frac{1}{l_r}\int_0^{l_r} \eta^2(x_i, y_i)dx} \tag{10}$$

where: lr denotes the sampling length and η denotes the distance of the sampling point from the mean plane. At the end of cutting, the surface profile of the workpiece x (185Å, 285Å) is extracted and the z-axis coordinates of the mean plane are computed to derive the distance of the sampling point from the mean plane η (xi, yi).

The results show that dg = 12.86 nm, the surface is relatively flat, the overall height distribution is uniform, there is almost no obvious microstructural features, indicating that the larger grain size of the material surface deformation is small, the lowest roughness; dg = 8.72 nm, the surface appeared slightly inhomogeneous, the

local height of the region fluctuations, but the overall is still relatively flat; dg = 7.35 nm, the surface roughness gradually increases, atomic steps gradually appear, the micro-morphology began to appear obvious undulation; dg = 6.51 nm, the surface height distribution is obviously uneven, the appearance of the "Atomic groove", indicating that when the grain size decreases, the plastic deformation in the cutting process is intensified, resulting in increased surface roughness. Dg = 5.93 nm, the surface appears slight inhomogeneity 5.93 nm, the surface shows more significant micro-undulation, there are obvious "Atomic steps" structure, the height distribution of non-uniformity reaches the maximum, the surface roughness increases significantly, reflecting the small grain size under the material deformation of the most prominent non-uniformity. As the grain size decreases, the surface roughness of the workpiece gradually increases, which is manifested by the enhancement of the height distribution inhomogeneity and the gradual obviousness of the atomic steps and groove structure. This suggests that grain size has a significant effect on surface quality and that materials with smaller grain sizes are more prone to micro-defects and height heave during the cutting process [18].

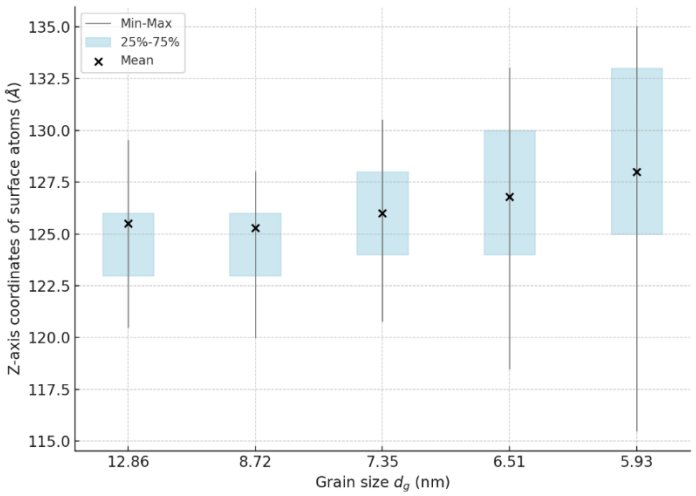

Figure 2. Statistical diagram of the Z-axis coordinate distribution of atoms on the machined surface.

The surface roughness of nano-cutting can be reduced to the emi level, so it can realize the ultra-high precision control of the size of machined parts. In order to quantitatively examine the influence of grain size on surface quality, the Z-axis coordinate distribution of the atoms on the machined surface is counted as shown in **Figure 2**, and the change rule of surface roughness Rq with grain size is shown in **Figure 3**. As the grain size decreases, the Z-axis coordinate distribution range of surface atoms becomes larger, and the surface roughness Rq gradually increases. When the grain size is 6.51 nm, the average rebound height of the machined surface is the lowest, and the surface morphology is atomic grooves; while the grain size is 5.93 nm, the average rebound height of the machined surface is the highest, and the surface morphology is atomic steps. This is because the workpiece grain size decreases, the grain size increases, the grain boundary increases; the mechanical properties of different grains on both sides of the grain boundary are different, and the processing resilience is also different, resulting in the formation of more atomic steps and grooves

after processing, and the surface quality decreases.

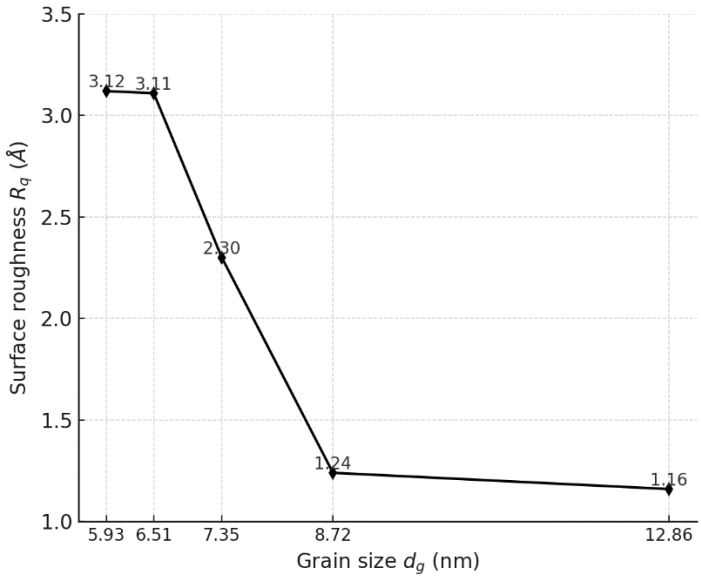

Figure 3. Effect of grain size on workpiece surface roughness.

Considering the two grain sizes of 6.51 nm and 5.93 nm, although they have some research value, due to the further grain refinement, the surface morphology has already shown significant Atomic grooves and Atomic steps, and its high degree of inhomogeneity reaches the peak, showing obvious extreme features. Therefore, the mechanical properties of the three grain sizes, 12.86 nm, 8.72 nm and 7.35 nm, are further compared.

The interplay between grain size and material properties is governed by the Hall-Petch relationship and mechanosensing pathways. The Hall-Petch relationship establishes that as grain size decreases, the increased density of grain boundaries hinders dislocation motion, resulting in enhanced material strength (modulus of elasticity) but reduced toughness due to limited plastic deformation [19]. Simultaneously, mechanosensing pathways highlight the biological perspective, where material properties like grain size influence cellular responses through mechanotransduction processes. These pathways convert mechanical stimuli into biochemical signals, affecting cell adhesion, proliferation, and differentiation via focal adhesion complexes and the cytoskeleton. Together, these frameworks provide a theoretical foundation for understanding how material microstructure influences both mechanical performance and cellular behavior, as quantified by the Hall-Petch equation below:

$$\sigma_y = \sigma_o + kd_g^{-0.5} \tag{11}$$

where σ_y is the material strength and d_g is the grain size. When the grain size decreases, dislocation motion is more easily captured by grain boundaries, leading to enhanced plasticity. Fine grains enhance strength, but lead to weaker deformation and exhibit reduced toughness.

4. Analysis of cellular responses

4.1. Material selection

From the previous analysis, it can be seen that the material with a grain size of 12.86 nm exhibits excellent mechanical properties, and the modulus of elasticity is lower at larger grain sizes, indicating that the material has moderate stiffness, which is closer to the mechanical properties of natural tissues. For biomaterials, the mechanical properties are closely related to cell behavior, and too high stiffness may adversely affect cell proliferation and attachment. The material at this grain size has optimal fracture resistance and ductility, which is beneficial in providing more uniform and stable surface properties during cell contact, preventing microscopic crack extension and enhancing the biosafety of the material. The lower amount of plastic deformation ensures the structural stability of the material during the experimental process and avoids affecting the accuracy of the experimental results due to excessive deformation.

In the nano-cutting experiments, the surface of the workpiece with a grain size of 12.86 nm exhibits optimal roughness. Compared to smaller grain sizes, the surface of the 12.86 nm material is more homogeneous, with fewer defects and virtually no visible atomic steps or atomic grooves, which significantly reduces the inhomogeneous mechanical stimulation of the cells when they come into contact with the surface. The large grain size results in a lower density of grain boundaries, less hindered dislocation motion, and a more stable surface quality, which is conducive to uniform cell attachment and spreading. The smooth and uniform surface microstructure helps fibroblasts form a more stable adhesion interface on the material surface, providing ideal cell growth conditions. Surface quality is a key factor influencing cell behavior, and excessive surface roughness can lead to uneven cell adhesion, while the 12.86 nm grain size provides an optimal solution for surface quality.

Compared to smaller grain sizes (e.g., 6.51 nm and 5.93 nm), the 12.86 nm material has higher stability, which helps to form a stable cell adhesion interface and reduces the risk of material fragmentation, ensuring the safety and stability of cell proliferation experiments. Moderate modulus of elasticity: it can provide cells with a mechanical microenvironment similar to natural matrix and promote normal biological behavior of cells. Low surface roughness: conducive to the uniform attachment of cells and reduce the interference of mechanical stimuli on cell behavior. Therefore 12.86 nm grain size polycrystalline tantalum nanomaterials were chosen for the next experiments [20].

Other materials: six-well plate, Flexcell; human skin fibroblasts (HFF-1), Shanghai Cell Bank, Chinese Academy of Sciences; high glucose medium (glutamine-free), fetal bovine serum (FBS), cell counting kit (CCK-8 kit), Yisheng Biotech, Shanghai; EasyScript® One- Step gDNA Removal and cDNA Synthesis SuperMix, Beijing Quanshijin Biological Company. EasyScript® One- Step gDNA Removal and cDNA Synthesis SuperMix, Beijing QuanShiJin Biological Company.

Human skin fibroblasts are highly adaptable in vitro, easy to culture and pass on, and have a fast proliferation rate, which can provide the required number of cells for

experiments in a relatively short period of time [21]. The stable biological properties of fibroblasts contribute to the reproducibility of the experiments and ensure the accuracy and reliability of the data. Fibroblasts are extremely sensitive to parameters such as surface morphology, mechanical properties, and biocompatibility of materials, making them ideal model cells for assessing the biological properties of materials. In addition, human skin fibroblasts have a direct physiological correlation with human skin tissues, making them a higher clinical reference value in biomedical research. Therefore, human skin fibroblasts were chosen.

Studies have shown that nanoscale surface roughness affects cell adhesion, which is a prerequisite for the survival, growth and proliferation of adherent cells on the substrate, and therefore nanoscale roughness has an important influence on cell proliferation and differentiation. The surface roughness of the samples was analyzed by an atomic force microscope (AFM) (Keysight 5500AFM-SPM, USA) with a scanning area of 25 μm × 25 μm.

4.2. Experimental procedure

Sterilized samples and cells (12×104 mL^{-1}) were pre-cultured in 6-well plates for 72 h, and then cultured for 1 and 3 d for the cell proliferation test. The medium was changed every 48 h, and the cell proliferation assay was carried out using the CCK-8 method, and the absorbance at 450 nm was read. It was found that the proliferation of HFF-1 cells in contact with polycrystalline tantalum nanomaterials and without contact with polycrystalline tantalum nanomaterials was pre-cultured for 72 h and then cultured for 1 and 3d as shown in **Figure 4**. The absorbance of all the scaffolds increased with time, indicating that the polycrystalline tantalum nanomaterials had good biocompatibility and supported the growth of HFF-1 cells. In addition, the fibroblasts on polycrystalline tantalum nano showed a proliferative trend, and their absorbance at 1 and 3 d was 1.67 and 1.5 times higher than that of the blank control group, respectively. The good proliferation-activating effect of polycrystalline tantalum nanomaterials on fibroblasts was confirmed.

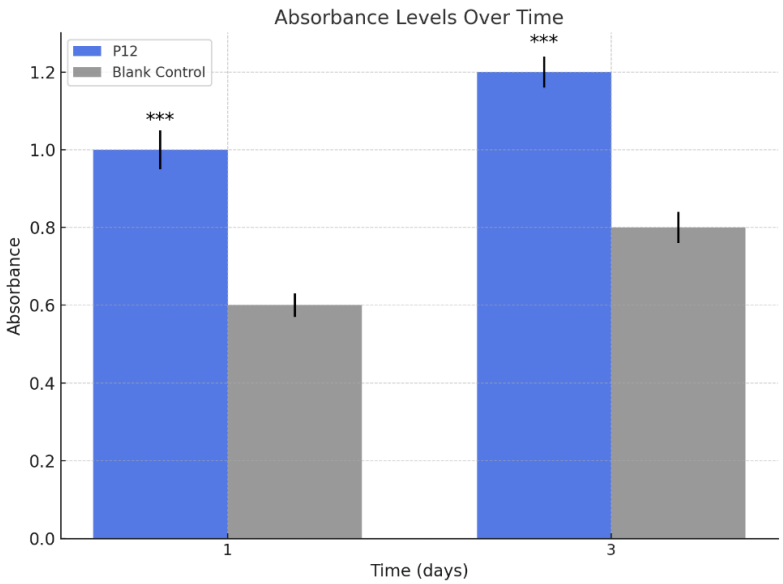

Figure 4. Trend of absorbance.

5. Further simulation experiments

5.1. Materials and methods

Adherence to ethical guidelines is crucial in biological experiments, especially when animal or human samples are involved. In order to ensure that experiments are ethical and conducted without violating animal protection or biosafety regulations, we have adopted simulated environments as an alternative to experiments. In this way, we are able to replicate the complexity and diversity of the in vivo environment as much as possible without directly involving real organisms, thus obtaining experimentally valuable data. The wide application of this simulation experiment method is in line with the guiding principles of the International Bioethics Review Committee (IBC) and the requirement of ethical responsibility in modern biomedical research, providing a sustainable solution to promote scientific research and innovation.

Cells and main reagents: L929 mouse fibroblasts (provided by the laboratory of North China University of Science and Technology, School of Stomatology). Pure hydrogenated titanium powder, pure zirconium powder, pure niobium powder, pure molybdenum powder, pure tantalum powder, anhydrous ethanol, sodium stibogluconate, RPMI 1640 (Corning, USA), PBS and trypsin (Biological Industries, Israel), fetal bovine serum (Cegrogen, Germany), MTT(3-(4,5-Dimethyl-2-thiazolyl)-2,5-diphenyltetrazolium Bromide (MTT) is a type of tetrazolium salt that changes to formazan when taken up into living cells) and DMSO(Dimethyl sulfoxide (DMSO) is a nonprotonic polar solvent capable of dissolving many organic and inorganic compounds, and is also a very safe solvent) (TCI, Japan), enzyme labeling instrument SM600 (Shanghai Yongchuang Medical Instrument Co., Ltd.),inverted phase contrast microscope Primovert (ZEISS, Germany) and field emission scanning electron microscope S-4800 (Hitach, Japan).

Specimen preparation: The alloy compositions were designed using the alloy cluster modeling theory. The Ti-27Nb-6Zr-5Mo alloy (titanium alloy specimen) was prepared by sintering at 1400 ℃ for 2 h using powder metallurgy; the nanooxidized layer was constructed on the surface of titanium alloy in situ using anodic oxidation method (oxidized layer specimen); and the tantalum coating was prepared on the surface of titanium alloy by plasma spraying method on the basis of the constructed oxidized layer to form the titanium alloy as the substrate, with the nanooxidized layer as the transition layer, and covered with polycrystalline tantalum nanocoating/titanium alloy coating specimen. The specimens were prepared as cylinders with a diameter of 10 mm and a thickness of 2 mm (provided by the laboratory of the School of Materials and Engineering, North China University of Science and Technology), and the surface morphology was observed under a scanning electron microscope.

Preparation of specimen extracts: Eight specimens were taken from each group, soaked in anhydrous ethanol for 30 min, cleaned with ultrasonic cleaner for 15 min, rinsed with deionized water, and sterilized by autoclave at 121 ℃ for 30 min. The specimens were put into 24-well plates, and then extracted with RPMI 1640 medium containing 10% fetal bovine serum as extraction medium at 37 ℃ for 72 h in an incubator of 5% CO_2, and the surface area of the specimens was 1.25 cm^2:1 mL. And the extract was filtered through 0.22 um membrane to remove bacteria and set aside.

MTT assay for cell proliferation: Logarithmic phase L929 cells were seeded at a density of 2000 cells per well in a 96-well plate, divided into 5 groups, with 4 wells per group. Each well was supplemented with 100 μL of cell suspension and cultured for 24 h. After the cells adhered, the titanium alloy group and the tantalum coating group were treated with the corresponding extract solution to replace the old culture medium. The negative control group was replaced with RPMI 1640 medium containing 10% fetal bovine serum (v/v), and the positive control group was replaced with a 0.6% phenol solution. The cells were incubated at 37 °C with 5% CO_2. On days 10, 20, and 30, cells were observed under an inverted phase contrast microscope to assess cell morphology. Then, 20 μL of MTT (5 g/L) was added to each well, and the cells were incubated for another 4 h. After removing the old culture medium, 150 μL of DMSO was added to each well. The plates were shaken for 15 min at room temperature, and the absorbance (*A*) value was measured using a microplate reader at 490 nm. The experiment was repeated 3 times.

Toxicological analysis: Relative cell proliferation rate (RGR) = (mean A value of experimental group/mean A value of negative control group) × 100%. According to the RGR, there are 5 grades: >99% is grade 0; 75% ～ is grade 1; 50% ～ is grade 2; 25% ～ is grade 3; 1% ～ is grade 4; ＜1% is grade 5. Grade 0 or 1 indicates low toxicity of the material; grade 2 should be combined with the morphology of the cells for a comprehensive toxicity analysis; and grades 3 to 5 indicate high toxicity of the material.

5.2. Results

The results of the experiment are as follows:

On the 10th, 20th and 30th days, the cells in the titanium alloy group and the tantalum-coated group were normal in morphology, polygonal, with well-defined nuclei and gradually increasing in number (**Table 1**).

Table 1. *A*-value of cells in each group.

Group	Day 10	Day 20	Day 30	*F*	*P*
Titanium group #	0.218 ± 0.03	0.448 ± 0.08	0.918 ± 0.07	99.049	< 0.001
Tantalum coating group #	0.229 ± 0.03	0.549 ± 0.06*	0.972 ± 0.09*	118.231	< 0.001
Negative control group #	0.252 ± 0.02	0.425 ± 0.04	0.773 ± 0.05	188.491	< 0.001
Positive control group	0.171 ± 0.01	0.179 ± 0.01	0.164 ± 0.01	2.463	0.140
F	6.386	20.350	94.374		
P	0.003	< 0.001	< 0.001		

Note: *: same time point, compared with the negative control group, $P < 0.05$; #: two-by-two comparison at different time points, $P < 0.05$

Titanium alloy and tantalum coating were both class 1 on day 1 and class 0 on days 20 and 30; the negative control was class 0; the positive control was class 2 on day 10, class 3 on day 20, and class 4 on day 30 (**Table 2**).

Table 2. RGR of cells in each group (%).

Group	Day 10	Day 20	Day 30
Titanium group	86.5	105.4	118.8
Tantalum coating group	90.9	129.2	125.7
Negative control group	100.0	100.0	100.0
Positive control group	67.9	42.1	21.2

The cell morphology of both the titanium alloy group and the tantalum-coated group remained normal during the experimental period, with a clear nucleus morphology and a gradual increase in the number of cells. Especially on the 30th day, the cell proliferation level of the tantalum-coated group was significantly higher than that of the titanium-alloyed group, indicating that the tantalum coating had a strong ability to promote cell proliferation. According to the analysis of absorbance value (*A*-value) of MTT method, the cell proliferation level of tantalum-coated group was higher than that of titanium alloy group at all time points, and the statistical difference was significant on the 20th and 30th days, indicating that tantalum showed superior effect in cell growth and division.

Secondly, in the toxicity analysis, both the titanium alloy group and the tantalum-coated group showed low toxicity (RGR $\geq$ 75%), demonstrating good biocompatibility, while the positive control group (containing 0.6% phenol solution) showed high toxicity, proving that tantalum-coated biosafety is much superior compared to conventional loading materials. This result highlights the potential of tantalum in reducing toxic reactions associated with implanted materials.

In terms of cellular responses in the long-term experiments, the cell proliferation rates of the titanium and tantalum-coated groups gradually increased, but the tantalum-coated group showed a higher cell proliferation rate than the titanium group at all time points. In particular, on day 20, the cell proliferation rate of the tantalum-coated group reached 129.2%, which was significantly higher than that of the titanium alloy group, which was 105.4%. These results suggest that tantalum coating not only promotes cell growth, but may also provide better support for tissue repair in long-term use.

6. Conclusions and recommendations

6.1. Research conclusions

In this study, the mechanical properties of polycrystalline tantalum nanomaterials with different grain sizes and their effects on the behavior of human skin fibroblasts were investigated in depth through molecular dynamics simulations and cellular experiments, and the following systematic conclusions were drawn:

First, the grain size has a significant effect on the mechanical properties of polycrystalline tantalum nanomaterials. Molecular dynamics cutting simulation results show that polycrystalline tantalum nanomaterials with larger grain size (e.g., 12.86 nm) have more superior mechanical performance, as evidenced by more stable stress-strain curves, moderate elastic modulus, and significantly higher elongation at break and toughness. This indicates that the material has stronger fracture resistance and plasticity under larger deformation, which results in better structural stability and

compressive strength when subjected to external loads. This improvement in mechanical properties may be mainly attributed to the reduction of grain boundary density under larger grain size, which reduces the hindering effect of grain boundaries on dislocation movement, leading to more uniform plastic deformation and reducing the local stress concentration caused by dislocation accumulation.

Secondly, the surface quality shows significant difference under different grain sizes. The larger the grain size, the lower the surface roughness of the material, which is characterized by higher flatness and microscopic uniformity. Surface defects (e.g., atomic steps, atomic grooves) were significantly reduced for materials with larger grain sizes, which provided a more ideal microscopic environment for cell adhesion, spreading, and proliferation. In addition, the enhanced surface flatness reduces the uneven mechanical stimulation of cells on the material surface, resulting in more stable cell behavior and higher proliferation efficiency.

Further, the effects of materials with different grain sizes on the behavior of fibroblasts were verified by cellular experiments, and it was found that the material with larger grain size (12.86 nm) could significantly promote the adhesion, proliferation and expansion of fibroblasts. This is mainly attributed to the fact that the larger grain size materials have both appropriate mechanical properties and surface quality: the moderate elastic modulus is closer to the mechanical environment of natural tissues, which provides a mechanical microenvironment for the normal growth of fibroblasts; and the flat surface reduces the risk of localized stress concentration and distortion of the cellular morphology, which strengthens the interfacial adhesion between the cells and the materials. In addition, the stability of the material microstructure reduces the experimental uncertainty due to local grain boundary effects and defects, resulting in a more uniform and controllable cell behavior.

In summary, polycrystalline tantalum nanomaterials with larger grain sizes exhibit dual advantages in terms of mechanical properties and biocompatibility, specifically higher toughness and compressive strength, lower surface roughness, and stronger cell proliferation promotion ability. This result reveals an important correlation between the mechanical properties of the materials and the cellular behavior, providing a theoretical basis for a deeper understanding of the mechanism of biomaterial-cell interaction. The present study further demonstrates that optimizing grain size can effectively regulate the surface microstructure and macroscopic mechanical properties of materials, thus improving their biological properties, especially in the field of tissue engineering and repair, which shows a broad application prospect. In addition, this study provides scientific guidance for the design and development of tantalum-based biomedical materials in the future, emphasizing the importance of precisely controlling the grain size and grain boundary density at the material microscopic scale. By optimizing the mechanical properties and surface quality of the materials, tantalum nanomaterials can be efficiently applied in a variety of fields such as trauma repair, bone implants, skin tissue engineering, etc., providing new solutions for the development of high-performance biomaterials.

6.2. Suggested implications

This study provides important theoretical foundations and practical insights for

the application of polycrystalline tantalum nanomaterials in the biomedical field. First, the results highlight the importance of grain size optimization for the mechanical and biological properties of polycrystalline tantalum nanomaterials. Larger grain size materials (e.g., 12.86 nm) show dual advantages in mechanical stability and cell behavior modulation. Therefore, future material development should focus on the precise regulation of grain size to improve the toughness and biocompatibility of materials by optimizing the grain boundary density and microstructure, a strategy that can also be extended to other metal or alloy materials to provide universal guidance for the fine-tuned design of biomaterials.

Second, the mechanical properties of materials (e.g., modulus of elasticity, toughness, and surface roughness) directly affect cell behavior, especially cell proliferation, attachment, and migration. This study reveals that moderate elastic modulus and high flatness surface promote the behavior of fibroblasts, and suggests that the effects of other mechanical parameters (e.g., shear modulus, surface energy, etc.) on the behavior of multiple cell types should be further explored in the future. In addition, multi-scale simulation and experimental methods can be combined to investigate in depth the mechanism of material micromechanical properties and cell-material interface interactions, in order to construct a database of mechanical properties for biomaterial design.

In terms of applications, polycrystalline tantalum nanomaterials show great promise in tissue engineering and trauma repair. In particular, its outstanding performance in promoting fibroblast proliferation makes it an ideal scaffold material for skin trauma repair. Combined with its high toughness and compressive strength, the material can also be used in orthopedic implants, especially in areas that are subject to high loads, such as hip and knee joints. In addition, its surface flatness and biocompatibility make it suitable for use as a surface coating for medical implants, further enhancing antimicrobial properties and cellular adaptability. To realize these applications, it is recommended to optimize the physical, chemical and mechanical properties of tantalum-based materials for different medical needs and to promote their practical translation from laboratory research to clinical applications.

In order to improve the depth and breadth of the research, it is recommended that interdisciplinary cooperation be further strengthened in the future by combining technologies and theories from the fields of materials science, biomechanics, and cell biology. On the one hand, material design parameters can be optimized by high-precision simulation tools; on the other hand, the dynamic interactions at the material-cell interface can be investigated by combining high-resolution microscopy and multi-channel detection platforms. Meanwhile, long-term in vivo experiments are carried out to assess the degradation behavior, stability and biological functions of the materials in complex biological environments. In addition, to address the high cost and complex processing of tantalum materials, it is recommended to explore more cost-effective preparation methods, such as reducing the production cost through nanostructure optimization techniques or developing tantalum matrix composites to balance performance and economics.

6.3. Research shortcomings and prospects

This study has several limitations that offer opportunities for future research. First, while the focus on polycrystalline tantalum nanomaterials provides detailed insights into their mechanical and biological properties, the lack of comparative analysis with other biomaterials, such as titanium-based alloys or cobalt-chromium, limits the generalizability of the findings. Expanding material variability in future studies could offer broader insights into biomaterial optimization. Second, although in vivo validation was incorporated through 10-, 20-, and 30-day mouse control experiments, these assessments remain preliminary and confined to short-term evaluations. Long-term in vivo studies are essential to assess factors such as chronic immune responses, material degradation, and functional integration in complex biological systems. Third, while cell proliferation assays were extended to 10-, 20-, and 30-day intervals, the study remains limited in capturing long-term cellular behaviors, such as differentiation, migration, and apoptosis, which are critical for tissue engineering applications. Fourth, the study focuses on a relatively narrow range of grain sizes and provides only a preliminary exploration of the underlying mechanisms linking grain size to material performance. Future work should explore a broader range of grain sizes and their interactions with other mechanical and biological parameters, such as surface energy and hydrophobicity. Finally, while surface roughness measurements using AFM were complemented by additional scans to ensure consistency, inherent limitations in this method call for the integration of complementary techniques, such as 3D profilometry or high-resolution scanning electron microscopy, to provide more comprehensive surface characterization. Future research should adopt an interdisciplinary approach, combining advanced material fabrication, multi-scale simulations, and in-depth biological studies, to optimize biomaterial properties for applications such as trauma repair, bone implants, and soft tissue regeneration. By addressing these limitations, future studies can build on the current findings to enhance the design and applicability of tantalum-based biomaterials and related materials in biomedical fields.

Ethical approval: Not applicable.

Conflict of interest: The author declares no conflict of interest.

References

1. Yang Z, Zhu J, Lu B, et al. Powder bed fusion pure tantalum and tantalum alloys: From original materials, process, performance to applications. Optics & Laser Technology. 2024; 177: 111057.
2. Meyers M A, Mishra A, Benson D J. Mechanical properties of nanocrystalline materials. Progress in materials science. 2006; 51(4): 427-556.
3. Ifijen IH, Christopher AT, Lekan OK, et al. Advancements in tantalum based nanoparticles for integrated imaging and photothermal therapy in cancer management. RSC advances. 2024; 14(46): 33681-33740.
4. Levin M, Stevenson CG. Regulation of cell behavior and tissue patterning by bioelectrical signals: challenges and opportunities for biomedical engineering. Annual review of biomedical engineering. 2012; 14(1): 295-323.
5. Ligda JP. Effects of grain size on the quasi-static mechanical properties of ultrafine-grained and nanocrystalline tantalum. The University of North Carolina at Charlotte. 2013.
6. Hirel P. Atomsk: A tool for manipulating and converting atomic data files. Computer Physics Communications. 2015; 197: 212-219.
7. Derlet PM, Van Swygenhoven H. Atomic positional disorder in fcc metal nanocrystalline grain boundaries. Physical Review

B. 2003; 67(1): 014202.
8. Papanikolaou M, Salonitis K. Grain size effects on nanocutting behaviour modelling based on molecular dynamics simulations. Applied Surface Science. 2021; 540: 148291.
9. Zhao Y, Zhang Y, Liu RP. MD simulation of chip formation in nanometric cutting of metallic glass. Advanced Materials Research. 2012; 476: 434-437.
10. Tersoff J. Modeling solid-state chemistry: Interatomic potentials for multicomponent systems. Physical review B. 1989; 39(8): 5566.
11. Mishin Y, Lozovoi AY. Angular-dependent interatomic potential for tantalum. Acta materialia. 2006; 54(19): 5013-5026.
12. Thompson AP, Aktulga HM, Berger R, et al. LAMMPS-a flexible simulation tool for particle-based materials modeling at the atomic, meso, and continuum scales. Computer Physics Communications. 2022; 271: 108171.
13. Stukowski A, Bulatov VV, Arsenlis A. Automated identification and indexing of dislocations in crystal interfaces. Modelling and Simulation in Materials Science and Engineering. 2012; 20(8): 085007.
14. Shimizu F, Ogata S, Li J. Theory of shear banding in metallic glasses and molecular dynamics calculations. Materials transactions. 2007; 48(11): 2923-2927.
15. Liu Y, Cui X, Sun X, et al. Investigations into the effect of cutting speed on nano-cutting of metallic glass by using molecular dynamics simulation analysis. The International Journal of Advanced Manufacturing Technology, 2023, 127(11-12): 5253-5263.
16. Ren J, Yue H, Liang G, et al. Influence of tool shape on surface quality of monocrystalline nickel nanofabrication. Molecules. 2022; 27(3): 603.
17. Jiang J, Sun L, Ma H, et al. Influence mechanisms of tool geometry parameters on surface quality and subsurface damage in polycrystalline NiFeCr superalloys. The International Journal of Advanced Manufacturing Technology, 2023, 127(7): 3637-3653.
18. Ralston KD, Birbilis N. Effect of grain size on corrosion: a review. Corrosion. 2010; 66(7): 075005-075005-13.
19. Hansen N. Hall–Petch relation and boundary strengthening. Scripta materialia. 2004; 51(8): 801-806.
20. Ayrilmis N, Buyuksari U, As N. Bending strength and modulus of elasticity of wood-based panels at cold and moderate temperatures. Cold Regions Science and Technology. 2010; 63(1-2): 40-43.
21. Madelaire CB, Klink AC, Israelsen WJ, et al. Fibroblasts as an experimental model system for the study of comparative physiology. Comparative Biochemistry and Physiology Part B: Biochemistry and Molecular Biology. 2022; 260: 110735.